Environmental Science and Pollution Research (2019) 26:33067–33075
https://doi.org/10.1007/s11356-019-06301-9

RESEARCH ARTICLE

Investigation of low-temperature selective catalytic reduction of NO_x with ammonia over Cr-promoted Fe/AC catalysts

Tingting Ge[2] · Baozhong Zhu[1] · Yunlan Sun[1] · Weiyi Song[1] · Qilong Fang[2] · Yuxiu Zhong[2]

Received: 22 May 2019 / Accepted: 26 August 2019 / Published online: 12 September 2019

Abstract

Fe/activated coke (AC) and Cr-Fe/AC catalysts with AC as a supporter and Cr and Fe as active components were prepared by an impregnation method for low-temperature selective catalytic reduction (SCR) of NO with NH_3. The effects of Cr addition and its concentrations on the deNO_x performance of Fe/AC catalysts were studied at low temperature. The Cr addition promotes the low-temperature SCR activity of the 8Fe/AC catalyst and the 8Fe6Cr/AC catalyst has the best low-temperature SCR deNO_x performance, which the NO_x conversions are greater than 90% at 160–240 °C. The 8Fe6Cr/AC catalyst has good water resistance. However, when 100 ppm SO_2 was introduced into the reaction gas, its deNO_x efficiency drops to 45% at 180 °C. To clarify the specific effects of Cr addition on the NO_x conversions and sulfur poisoning, the Cr-Fe/AC catalysts were characterized by X-ray diffraction, BET, H_2 temperature-programmed reduction, NH_3 temperature-programmed desorption, X-ray photoelectron spectroscopy, and Fourier infrared spectroscopy. The addition of Cr into Fe/AC catalysts greatly increases the BET surface area and the number of weak and medium-strong acid sites on the catalyst surface and improves the ratio of Fe^{3+}/Fe^{2+}. These factors enhance the NO_x conversion of 8Fe/AC catalyst. The formed sulfates and hydrogen sulfates cover the active sites on the catalyst surface, which lead to the sulfur poisoning of the 8Fe6Cr/AC catalyst.

Keywords Fe · Active coke · Low-temperature SCR · Cr

Introduction

With the development of industry, air pollution becomes more and more serious. Nitrogen oxides (NO_x) as the main pollutants have attracted intense attention. The selection catalytic reduction (SCR) of NO_x by NH_3 is a widely used technology in commercial SCR systems to control NO_x emissions from stationary sources. V_2O_5-WO_3/TiO_2 is extensively used as the SCR denitrification catalyst in power plants (Topsoe 1994), and its optimum operating temperature range is 300–400 °C (Phil et al. 2008). To avoid the additional costs of reheating the flue gas, SCR unit is located upstream of the electrostatic precipitator and desulfurization tower (Liu et al. 2012). Flue gas contains a large amount of fly ash, K^+, Na^+, and SO_2 because it is not treated by the electrostatic precipitator and desulfurization tower (Tang et al. 2007). These can cause catalyst poisoning and accelerate catalyst deactivation. Therefore, a low-temperature SCR catalyst placed downstream of the electrostatic precipitator and desulfurizer is extraordinarily necessary (Yang et al. 2016a, b).

Carbon-based materials such as multi-walled carbon nanotubes (Huang et al. 2007; Luo et al. 2012; Pan et al. 2013), single-walled carbon nanotubes (Gorji 2015; Zhang et al. 2018), activated carbon (Kim et al. 2015; Lázaro et al. 2006), activated coke (AC) (Wang et al. 2014a, b; Lin et al. 2017; Huang et al. 2014; Gao et al. 2018), activated semi-coke (Wang et al. 2014a, b), and carbon-coated materials (Ouzzine

Highlights
- The 8Fe6Cr/AC catalyst has excellent low-temperature deNO_x performance.
- Promotional effects of Cr on the deNO_x performance were discussed.
- H_2O had less effect on the deNO_x performance of 8Fe6Cr/AC catalyst.
- The SO_2 poisoning mechanism of 8Fe6Cr/AC catalyst was revealed.

Responsible editor: Philippe Garrigues

✉ Baozhong Zhu
bzzhu@cczu.edu.cn

✉ Yunlan Sun
ylsun@cczu.edu.cn

[1] School of Petroleum Engineering, Changzhou University, Changzhou 213164, Jiangsu, China

[2] School of Energy and Environment, Anhui University of Technology, Maanshan 243002, Anhui, China

et al. 2008; Gao et al. 2011) as catalyst supporters attracted the attention of researchers owing to their large specific surface areas and developed pore structures. Especially, AC with high mechanical strength is more suitable to be used as the carrier of $deNO_x$ catalysts. Yang et al. used AC as a carrier and a pyrolusite as active component to prepare a series of low-temperature $deNO_x$ catalysts, which obtained 74.2% $deNO_x$ efficiency at 150 °C (Lin et al. 2017). Wang et al. (2017a, b) prepared a series of catalysts using activated semi-coke (ASC) as a carrier. The experimental results showed that the Ce/ASC catalyst had the highest $deNO_x$ efficiency at 300 °C, which the NO_x conversion was 80% and N_2 selectivity was 90%. Gao et al. (2018) found that AC-supported 6% Ce can effectively remove mercury from flue gas. Although there are some studies on AC as the carrier of $deNO_x$ catalysts, the $deNO_x$ efficiency will need to be improved, especially at low temperature.

The active component is another important factor that plays a crucial role in the SCR $deNO_x$ reaction. Transition metal oxides such as Fe (Klukowski et al. 2009; Skarlis et al. 2014), Cr (Chen et al. 2012), Ni (Gao et al. 2017), Mn (Yang et al. 2016a, b), and Cu (Gao et al. 2013) show excellent performance in the low-temperature SCR reaction of NO with NH_3, especially for Mn and Fe. Mn-based catalysts have weak SO_2 and H_2O resistance (Yang et al. 2016a, b). However, Fe-based catalysts have good SO_2 and H_2O resistance (Wang et al. 2016; Xing et al. 2017), so some studies concentrated on the $deNO_x$ performance of AC-supported Fe-based catalysts (Du et al. 2018; Wang et al. 2017a, b). However, the NO_x conversions of AC-supported Fe-based catalysts should be further improved at low temperature. Adding metallic oxides can enhance the SCR $deNO_x$ performance of catalysts at low temperature (Qiu et al. 2013). Therefore, it is necessary to study the modification of AC-supported Fe-based catalysts to improve their NO_x conversions. Cr has various valences such as Cr^{2+}, Cr^{3+}, Cr^{5+}, and Cr^{6+}, which is prone to the redox reactions. Some researchers found that Cr has a promoting effect on the $deNO_x$ catalysts (Amin et al. 2003; Chen et al. 2012; Yang et al. 2015). Chen et al. (2012) found that Cr can effectively improve the $deNO_x$ performance of Mn-based catalysts at 80–220 °C. However, there are few studies on the effect of Cr on the $deNO_x$ performance of Fe/AC catalyst at low temperature. Therefore, in this paper, a series of Cr-modified AC-supported Fe-based catalysts were prepared by an impregnation method. The SCR $deNO_x$ activities were tested at 120–240 °C. In addition, the SO_2 and H_2O resistance of Cr-modified AC-supported Fe-based catalyst was also studied. Furthermore, the catalysts were characterized by BET, XRD, XPS, temperature-programmed reduction of H_2 (H_2-TPR), temperature-programmed desorption of NH_3 (NH_3-TPD), and FTIR, and the $deNO_x$ and SO_2 poisoning mechanisms were discussed according to the experimental and characterization results.

Experimental

Catalyst preparation

AC provided by Ningxia Zhongyou Activated Carbon Co., Ltd. was used as a supporter. Ferric nitrate ($Fe(NO_3)_3{\cdot}9H_2O$) and chromium nitrate ($Cr(NO_3)_3{\cdot}9H_2O$) were used as metal precursors of Fe and Cr, respectively. Firstly, the AC was crushed and sieved into granules with 40–60 mesh. Then, 2-g AC particles, ferric nitrate (Fe, AC = 0.04–0.1), and chromium nitrate (Cr, AC = 0.04, 0.06, 0.08) with a moderate amount of deionized water were mixed and stirred for 2 h on a magnetic stirrer. After the impregnation, the mixtures were dried at 105 °C for 6 h, followed by calcination in muffle furnace at 250 °C for 5 h, and cooled down to room temperature. The prepared catalysts are designated as xFeyCr/AC, where x is the Fe and AC mass percentage ratio and y is the Cr and AC mass percentage ratio.

Catalytic activity

The $deNO_x$ activities of xFeyCr/AC were investigated in a fixed-bed quartz reactor (inner diameter 3.5 mm) with continuously flowing gas at atmospheric pressure. The reactant gas was composed of 400 ppm NO, 400 ppm NH_3, 5% O_2, 5% H_2O (when needed), and 100 ppm SO_2 (when needed), and N_2 was used as the balance. The total gas flow rate was 130 mL/min and the gas hourly space velocity (GHSV) was 10400 $cm^3\ g^{-1}\ h^{-1}$. NO_x concentrations in the inlet and outlet flue gas were analyzed by a multi-component online flue gas analyzer. The NO_x (NO and NO_2) conversion was calculated by the following equation:

$$NO_X\ \text{conversion}\ (\%) = \frac{(NO_X)_{in} - (NO_X)_{out}}{(NO_X)_{in}} \times 100\% \qquad (1)$$

where $(NO_x)_{in}$ and $(NO_x)_{out}$ are the concentrations of NO_x in the inlet and outlet, respectively.

Catalyst characterization

The specific surface area, pore volume, and pore size were measured by a Micromeritics ASAP 2020 analyzer (Micromeritics Instrument Corp., USA). Prior to BET measurement, all catalysts were dried for 6 h at 105 °C and then degassed under vacuum at 220 °C for 6 h. The surface areas of xFeyCr/AC catalysts were measured by nitrogen adsorption at − 196 °C and calculated by the BET equation.

The XRD patterns were recorded on a Rigaku Ultima IV powder diffractometer (Rigaku Ultima, Japan) with Cu Kα radiation (λ = 0.154056 nm) to examine the crystallinity and dispersity of components on the supporter. The scanning range (2θ) was 10–80° and the scanning rate was 20° min^{-1}.

The operating voltage was 40 kV and the applied current was 40 mA.

The XPS spectra of Fe(2p) and Cr(2p) were determined by an Escalab 250Xi X-ray electron spectrometer (Thermo Scientific, USA) using Al Kα X-ray as the radiation source.

The H_2-TPR and NH_3-TPD were determined by the ChemBET Pulsar TPR/TPD (Quantachrome instruments of America) in the temperature range of 50–800 °C.

The Fourier-transform infrared spectra (FTIR) was obtained by a FT-IR Nicolet IS10 (Thermo Scientific, USA).

Results and discussion

SCR DeNO$_x$ performance

The NO_x conversions of xFe/AC catalysts are shown in Fig. 1. The NO_x conversion of AC catalyst is only 15 % at 120 °C and changes little as the temperature increases. However, it increases with increasing the loading amount of Fe on AC catalyst. When the Fe content is 8%, the NO_x conversions of Fe/AC catalyst are the highest, which are 41% and 91% at 120 °C and 240 °C, respectively. This may be due to the addition of Fe which increases the specific surface area of the catalysts and the acid sites on the catalyst surface. However, the NO_x conversions of 8Fe/AC catalyst are still relatively low, so they were modified by the addition of Cr.

Figure 2 shows the NO_x conversions of the 8FeyCr/AC catalysts at different temperatures. The NO_x conversions first increase then decrease with increasing the addition amount of Cr. They reach the maximum values when the Cr content is 6%, which are 63% and 100% at 120 °C and 180 °C, respectively. Furthermore, the NO_x conversion remains 100% at 240 °C after 4 h. Cr has different valence states, which are favorable to the catalytic redox reaction, especially in low-temperature section (Koehler et al. 2010), so the NO_x conversions increase with increasing the addition amount Cr. While the Cr content reaches a certain amount and gathers on the surface of catalyst, the specific surface area and the number of acid sites can be reduced, so the activity of catalyst decreases.

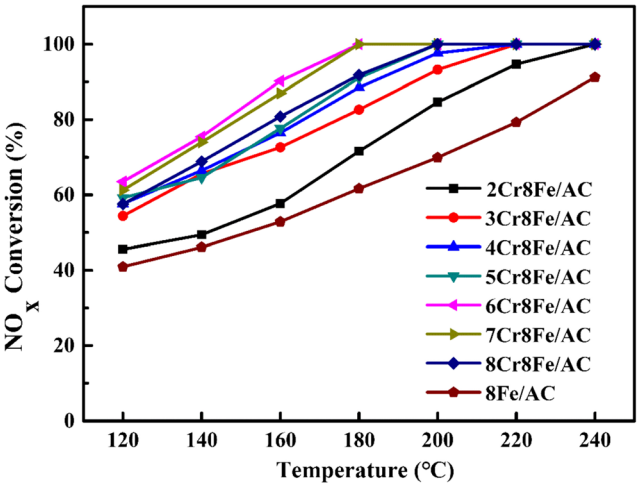

Fig. 2 NO_x conversions of the 8FeyCr/AC catalysts at 120–240 °C

To further understand the effects of Cr on the NO_x conversions of the 8Fe/AC catalyst, the NO_x conversions of the 8Fe/AC, 6Cr/AC, and 8Fe6Cr/AC catalysts were studied. The results are shown in Fig. 3. The NO_x conversions of the 8Fe/AC catalyst are higher than those of the 6Cr/AC catalyst, while the NO_x conversions of the 8Fe6Cr/AC catalyst have the highest, indicating that there is the interaction between Fe and Cr.

Effects of H_2O and SO_2

The effects of H_2O and SO_2 on the NO_x conversions of the 8Fe6Cr/AC catalyst were studied at 180 °C. The results are

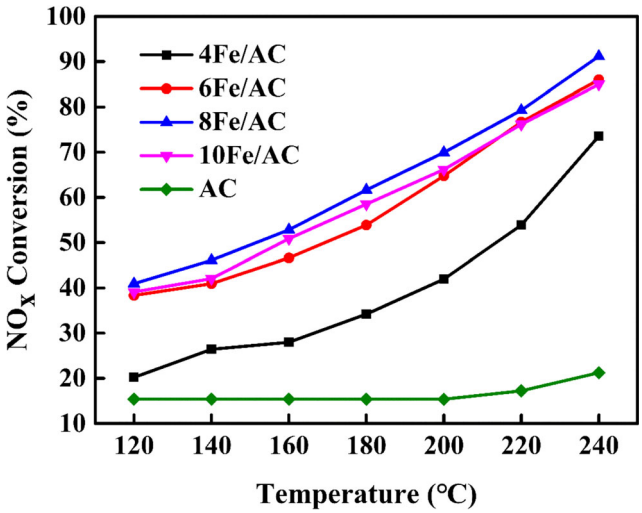

Fig. 1 NO_x conversions of the xFe/AC catalysts at 120–240 °C

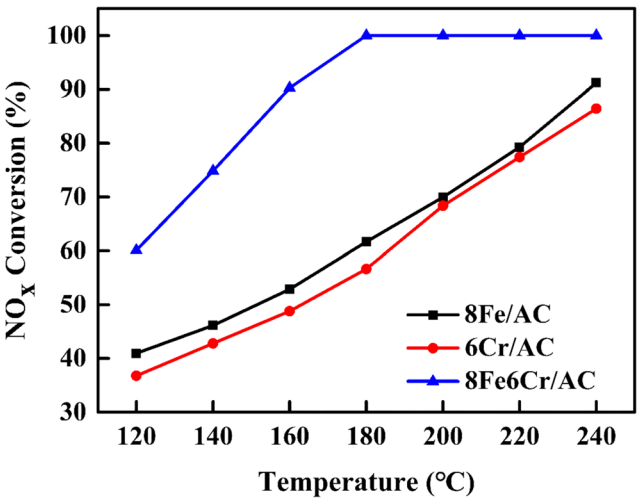

Fig. 3 NO_x conversions of the 8Fe/AC, 6Cr/AC, and 8Fe6Cr/AC catalysts at 120–240 °C

shown in Fig. 4. When H_2O or SO_2 were added to the reaction gas, the NO_x conversions did not immediately decrease because it took a certain time for the reaction gas to arrive at the gas analyzer and catalyst poisoning caused by H_2O or SO_2 requires a process. As shown in Fig. 4a, the NO_x conversion dropped from 100 to 73% after adding 5% H_2O. Removing the H_2O, the NO_x conversion restored to 93%, indicating that the 8Fe6Cr/AC catalyst has a certain H_2O resistance. The effect of SO_2 on the NO_x conversions of the 8Fe6Cr/AC catalyst is shown in Fig. 4b. When 100 ppm SO_2 was introduced into the reaction gas, the NO_x conversion dropped to 45%. After removing SO_2, the NO_x conversion did not restore, indicating that SO_2 reacts with NH_3 to form ammonium sulfate or ammonium hydrogen sulfate, which deposits on the surface of the catalyst and covers the active sites on the surface of the catalyst, so the NO_x conversions of the 8Fe6Cr/AC catalyst decrease.

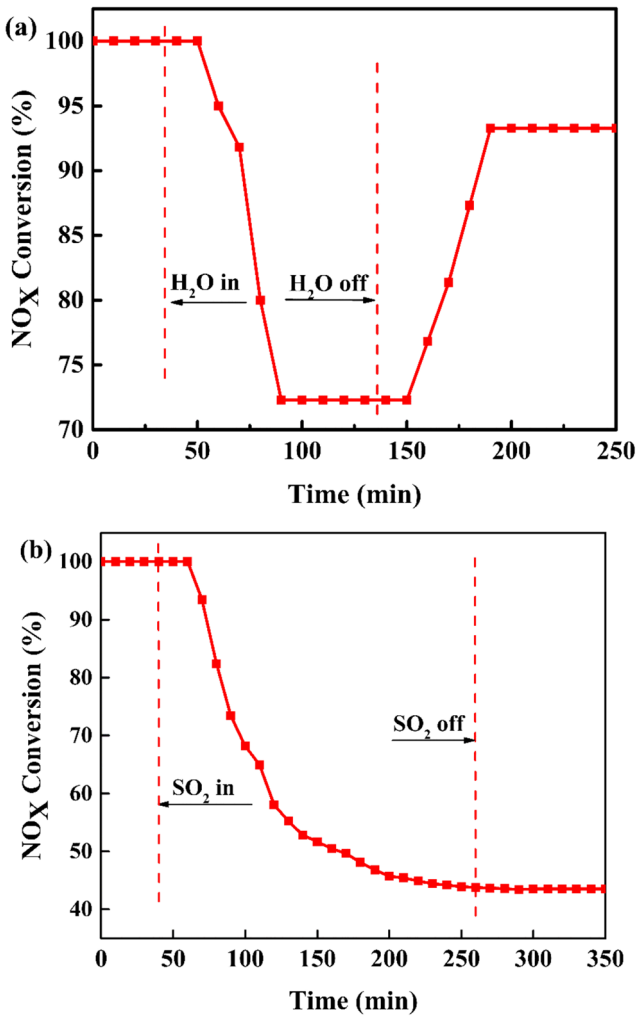

Fig. 4 Effects of H_2O (**a**) and SO_2 (**b**) on the NO_x conversions over the 8Fe6Cr/AC at 180 °C. Reaction conditions: $[NH_3] = [NO] = 400$ ppm, $[SO_2] = 100$ ppm, $[H_2O] = 5\%$, and GHSV = 10400 $cm^3\ g^{-1}\ h^{-1}$

Catalytic characterization

BET and XRD

The surface area, pore volume, and pore size of the xFeyCr/AC catalysts are summarized in Table 1. The surface area of AC is 163.2927 $m^2\ g^{-1}$. While loading Fe on AC, its surface areas and pore volumes increase, so the activities of the catalysts increase. The specific surface area of the 8Fe/AC catalyst is similar to those of the 6Fe/AC and 10Fe/AC catalysts, but it is not the largest in these three catalysts, indicating that although the surface area of catalyst has effects on the NO_x conversions, it is not a decisive factor. The specific surface area is further increased when Cr is added into the 8Fe/AC catalyst. With increasing the additional amount of Cr, the specific surface areas of the xFeyCr/AC catalysts first increase and then decrease owing to the excessive Cr gathering on the catalyst surface. The 8Fe6Cr/AC catalyst obtains the maximum specific surface area, so its deNO_x efficiency is the highest.

The crystalline phases of active components in these catalysts were examined by XRD and the results are shown in Fig. 5. A broad band in the range of 17–33° is found in the AC catalyst, corresponding to the amorphous carbon structure (Wang et al. 2017a, b). In addition, the characteristic peaks of the AC catalyst at 20.81°, 26.6°, 36.26°, 44.08°, 50.12°, 59.96°, and 68.04° correspond very well to the standard PDF card (ICDD, #46-1045), which belong to the SiO_2. With the addition of Fe and Cr in the AC catalyst, the intensity of the diffraction peaks of SiO_2 and carbon structure constantly weakens and no new diffraction peaks appear in the XRD spectrum, indicating that Fe and Cr are amorphous and have excellent dispersion on the catalyst surface. At the same time, the presence of Fe and Cr makes the original carbon and SiO_2 disperse on the catalyst surface. This is the reason that the BET specific surface areas of xFeyCr/AC catalysts increase.

Table 1 Physical properties of different catalysts

Catalyst	Surface area ($m^2\ g^{-1}$)	Pore volume ($cm^3\ g^{-1}$)	Average pore size (nm)
AC	163.2927	0.112315	4.8042
4Fe/AC	182.8739	0.136160	4.1312
6Fe/AC	195.4689	0.130489	3.6219
8Fe/AC	192.0318	0.130957	3.5877
10Fe/AC	193.3546	0.132523	3.7048
8Fe4Cr/AC	190.9599	0.121940	2.7102
8Fe6Cr/AC	209.2407	0.130809	2.3883
8Fe8Cr/AC	176.9851	0.110998	2.6786

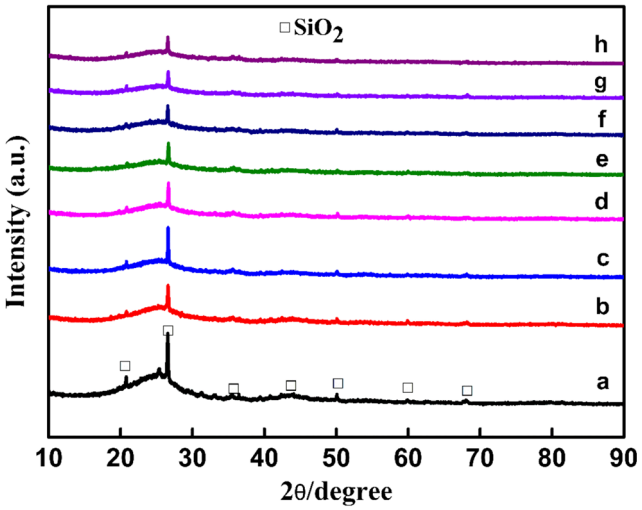

Fig. 5 XRD patterns of the catalysts (a) AC; (b) 4Fe/AC; (c) 6Fe/AC; (d) 8Fe/AC; (e) 10Fe/AC; (f) 8Fe4Cr/AC; (g) 8Fe6Cr/AC; and (h) 8Fe8Cr/AC

XPS

The surface chemical states of Fe, Cr, and O species for the xFeyCr/AC catalysts are shown in Fig. 6. Figure 6a shows the Fe 2p XPS spectra of the 8Fe/AC, 8Fe4Cr/AC, 8Fe6Cr/AC, and 8Fe8Cr/AC catalysts. The two characteristic peaks located at 709–716 eV and 723–729 eV correspond to the orbitals of Fe $2p_{3/2}$ and Fe $2p_{1/2}$, respectively. Fitting the Fe $2p_{3/2}$ spectra, the spectra of Fe^{2+} (peak at about 710.9 eV) and Fe^{3+} (peak at about712.8 eV) are obtained. Adding of Cr into the 8Fe/AC, the Fe $2p_{3/2}$characteristic peak shifts to the low binding energy, indicating that the interaction can happen between Fe and Cr. The binding energy is high, indicating that the element is more stable, while the binding energy is low, demonstrating that the element is more active (Shen et al. 2014). The contents of Fe^{2+}, Fe^{3+}, and the ratios of Fe^{3+}/Fe^{2+} are shown in Table 2. Compared with the 8Fe/AC catalyst, the Fe^{2+}contents of the 8Fe6Cr/AC catalyst decrease from 18.83 to 14.05% and the Fe^{3+}contents increase from 28.13 to 30.53%, indicating that adding a certain amount (6%) of Cr to the 8Fe/AC catalyst can increase the content of Fe^{3+} and decrease the content of Fe^{2+}. Increasing the amount of Cr from 6 to 8%, the contents of Fe^{2+} increase from 14.05 to 18.24% and the contents of Fe^{3+} decrease from 30.53 to 27.28%. This indicates that excessive Cr can increase the concentration of Fe^{2+} and reduce the concentration of Fe^{3+}. High valence metallic ions are favorable for the adsorption of NO on the catalyst surface and the oxidation of NO (Wang et al. 2015). Low-temperature SCR reaction is a complex process, and one of the main reaction paths is NH_3 adsorbing at the Brønsted acid site on the catalyst surface to form NH_4^+ ions, which then reacts with NO_2 to form H_2O and N_2 (Lin et al. 2004). Therefore, to some extent, the oxidation rate of NO to NO_2 can determine the NO_x conversion in the low-temperature SCR reaction. For the 8Fe6Cr/AC catalyst, the high ratio of Fe^{3+}/Fe^{2+} is one of the reasons for its high deNO_x activity at low temperature.

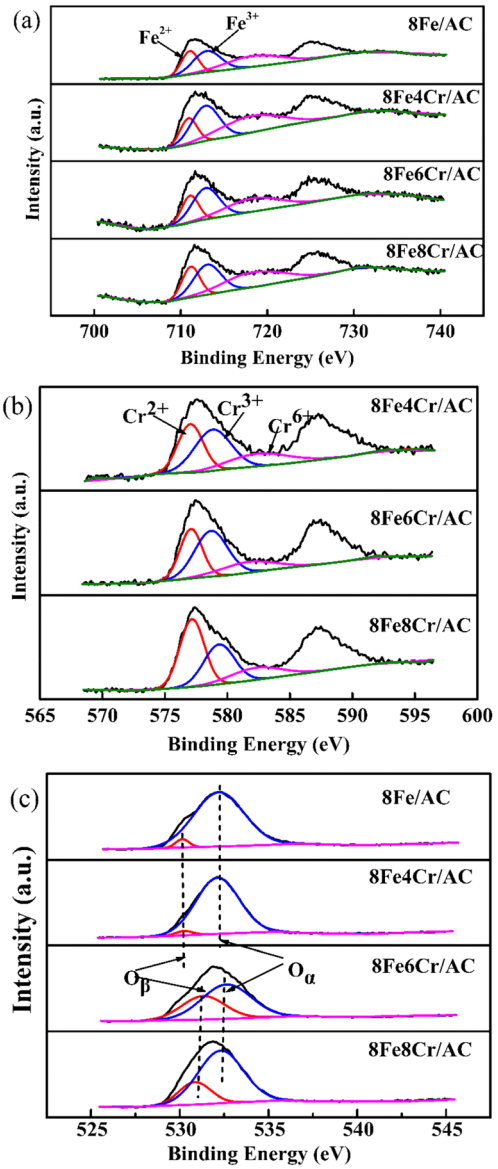

Fig. 6 XPS spectra of Fe (**a**), Cr (**b**), and O (**c**) for the 8Fe/AC, 8Fe4Cr/AC, 8Fe6Cr/AC, and 8Fe8Cr/AC catalysts

Figure 6b shows the Cr 2p XPS spectra of the 8Fe4Cr/AC, 8Fe6Cr/AC, and 8Fe8Cr/AC catalysts. Two characteristic peaks at 574–583 eV and 584–593 eV assigned to Cr $2p_{3/2}$ and Cr $2p_{1/2}$ are observed (Amin et al. 2003). Cr $2p_{3/2}$ spectrum is split into three peaks. They are Cr^{2+} (577.1 eV), Cr^{3+} (578.8 eV), and Cr^{6+} (582.4 eV). The contents of Cr^{2+}, Cr^{3+}, and Cr^{6+} are summarized in Table 2. The ratios of Cr^{3+}/Cr^{2+} are 1.21, 1.37, and 0.97 for the 8Fe4Cr/AC, 8Fe6Cr/AC, and 8Fe8Cr/AC catalysts, respectively. The 8Fe6Cr/AC catalyst has the highest ratio of Cr^{3+}/Cr^{2+}, indicating that Cr^{3+} has obvious promotion effects on the deNO_x performance. This result is consistent with the study of Wang et al. (2017a, b).

Table 2 Surface valence-state ratios of catalysts

Catalyst	Fe^{2+} (%)	Fe^{3+} (%)	Fe^{3+}/Fe^{2+}	Cr^{2+} (%)	Cr^{3+} (%)	Cr^{6+} (%)	Cr^{3+}/Cr^{2+}	O_β (%)	$O\alpha$ (%)	O_β/O_α
8Fe/AC	18.83	28.13	1.49					3.01	96.98	0.03
8Fe4Cr/AC	14.02	30.38	2.17	23.33	28.33	14.29	1.21	3.93	96.06	0.04
8Fe6Cr/AC	14.05	30.53	2.17	22.57	30.99	12.01	1.37	46.83	53.16	0.88
8Fe8Cr/AC	18.24	27.28	1.50	29.61	28.86	3.09	0.97	22.89	77.10	0.29

The content of Cr^{6+} in the 8Fe6Cr/AC catalyst is slightly lower than that in the 8Fe4Cr/AC catalyst, but its deNO_x efficiency is much higher than that in the 8Fe4Cr/AC catalyst, indicating that although the Cr^{6+} content has effects on the NO_x conversions, it is not a decisive factor.

The O 1s XPS is shown in Fig. 6c. It is divided into two peaks at 531.12 and 532.28 eV, which are assigned to the binding energies of the chemisorbed oxygen (O_β) (Wang et al. 2017a, b; Wu et al. 2011) and lattice oxygen (denoted as O_α) belonging to the Si–O bond in AC framework (Zhu et al. 2015), respectively. The surface contents of O_β and O_α, and the ratio of O_β/O_α are shown in Table 2. Compared with the 8Fe/AC catalyst, the ratios of O_β/O_α in the 8Fe6Cr/AC and 8Fe8Cr/AC catalysts increase from 0.03 to 0.88 and 0.29, respectively, indicating that the O_β content increases after the addition of Cr. O_β has better reaction activity than O_α (Shen et al. 2011), so the 8Fe6Cr/AC catalyst has excellent NO_x conversions.

H_2-TPR

H_2-TPR experiments were carried out to get insights into the redox properties of the different catalysts. Figure 7 shows the H_2-TPR results of the catalysts. There are two peaks in the AC catalyst. The peak at 458.41 °C can be the reduction peak of metal oxides in AC itself. The peak at 661.19 °C is attributed to the reduction peak of oxygen-containing functional groups (Ding et al. 2017). However, after loading Fe, the reduction peak of metal oxides in AC is covered by the peak at 437.93 °C, which is assigned to the reduction of Fe^{3+} to Fe^{2+} (Yang et al. 2013, 2011) due to the high Fe content. It can be observed that the reduction peak temperature of Fe^{3+} to Fe^{2+} gradually shifts toward a low temperature when Cr is added, indicating that Cr can lower the reduction temperature of the xFeyCr/AC catalysts. In addition, a new reduction peak appears at 321.87, 305.96, and 308.04 °C for 8Fe4Cr/AC, 8Fe6Cr/AC, and 8Fe8Cr/AC, respectively, which assigns to the reduction of Cr^{3+} to Cr^{2+} (Yang et al. 2015). The peak temperature represents the catalyst reducibility. The lower the peak temperature is, the stronger is the catalyst redox ability (Liu et al. 2008). Comparing these catalysts, it can be found that the 8Fe8Cr/AC catalyst has the lowest reduction peak temperature, indicating that it has the best catalytic activity. However, we do not find the reduction peak of Cr^{6+} in the catalysts. Therefore, the effects of Cr^{6+} on the redox ability of the xFeyCr/AC catalysts are negligible. This result is also supported by the XPS analysis. It can be also found from Fig. 7 that the addition of Cr into the 8Fe/AC catalyst increases the reduction peak area of Fe^{3+} to Fe^{2+}, indicating that

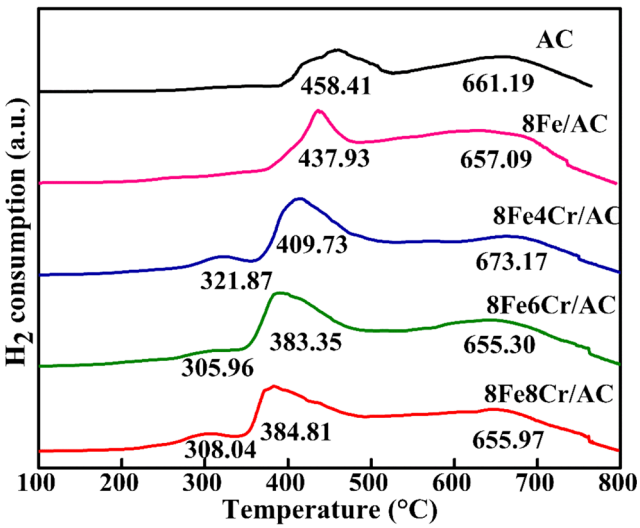

Fig. 7 H_2-TPR profiles of the catalysts

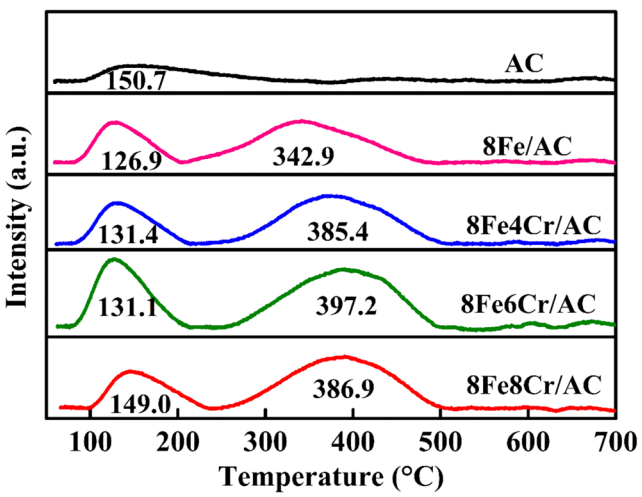

Fig. 8 NH_3-TPD profiles of the catalysts

the amount of reduced Fe^{3+} increases, so the NO_x conversions of these catalysts increase significantly.

NH_3-TPD

NH_3-TPD experiments were performed to determine the acid site distributions on the surfaces of the AC, 8Fe/AC, 8Fe4Cr/AC, 8Fe6Cr/AC, and 8Fe8Cr/AC catalysts. The results are shown in Fig. 8. The AC catalyst has only a broad desorption peak at 150.7 °C, corresponding to the NH_3 desorption from weak acid sites (Lewis acid sites) and physisorbed NH_3 (Yang et al. 2016a, b; Ding et al. 2017). Adding Fe into the AC catalyst, a new peak at 250–500 °C appears, which attributes to the NH_4^+ desorption from medium and strong acid sites (Brønsted acid sites) (Vishwanathan et al. 2004). Compared with the AC catalyst, the intensity of weak acid sites in the 8Fe/AC catalyst increases obviously, suggesting that the addition of Fe enhances the concentration of weak acid sites and adds a new medium and strong acid site to the catalysts. Adding Cr into the 8Fe/AC catalysts, the species of acid sites in xFeyCr/AC catalysts are not changed.

The desorption peak area of NH_3 represents the number of acid sites in the catalyst (Zhu et al. 2017). To determine the concentration change of acid sites, the number of Lewis acid sites and Brønsted acid sites of the catalysts was calculated and the results are shown in Fig. 9. Adding Fe into the AC catalyst, the number of both Lewis acid sites and Brønsted acid sites increases. When Cr modified the 8Fe/AC catalyst, the number of Lewis acid sites and Brønsted acid sites firstly increases then decreases. The 8Fe6Cr/AC catalyst has the largest amount of the acid sites, indicating that its catalytic activity is the highest. In addition, the number of Brønsted acid sites in 8Fe6Cr/AC catalyst is significantly higher than that of the Lewis acid sites, which shows that the Brønsted acid sites play the main role in the SCR deNO$_x$ reaction. There

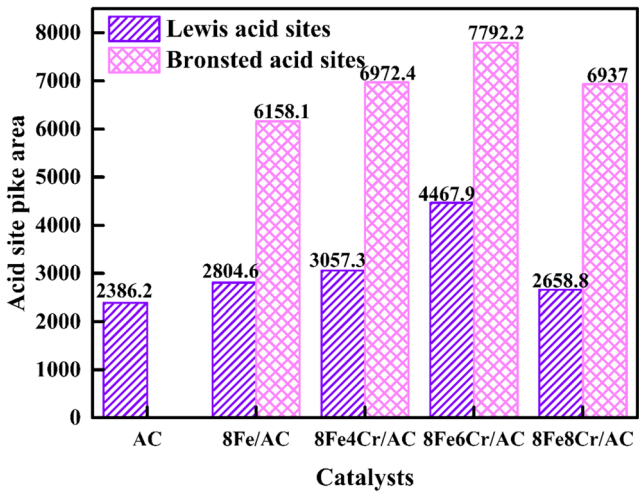

Fig. 9 Lewis acid site and Brønsted acid site comparison for different catalysts

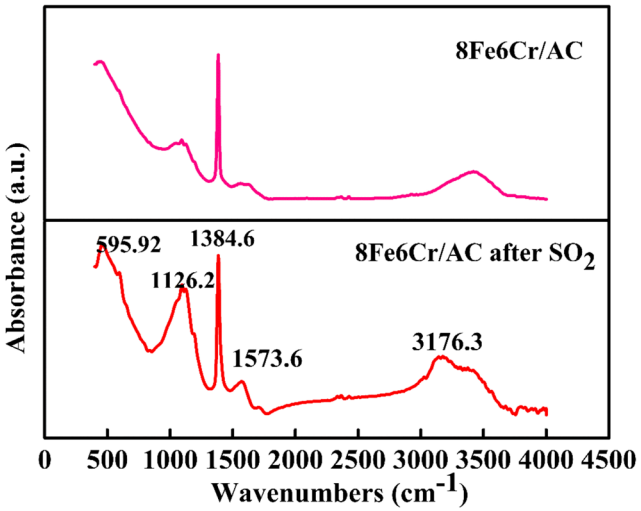

Fig. 10 FTIR spectra of the 8Fe6Cr/AC and 8Fe6Cr/AC poisoned by SO_2

are two main mechanisms such as E-R mechanism and L-H mechanism (Yang et al. 2016a, b), in which E-R mechanism mainly occurs at Lewis acid sites and L-H mechanism mainly occurs at Brønsted acid sites (Gao et al. 2013). For the 8Fe6Cr/AC catalyst, Lewis acid sites and Brønsted acid sites exist simultaneously, which indicates that the E-R mechanism and L-H mechanism co-exists in the NH_3-SCR reaction at low temperature.

FTIR

To clarify the reason for SO_2 poisoning of the 8Fe6Cr/AC catalyst, the fresh catalyst and the catalyst poisoned by SO_2 were studied by FTIR, and the results are shown in Fig. 10. Compared with the fresh 8Fe6Cr/AC catalyst, the 8Fe6Cr/AC catalyst poisoned by SO_2 shows new peaks at 595, 894, 1049, 1030, and 1080 cm^{-1}, which correspond to the moderate absorption peak of hydrogen sulfate, the weak absorption peak of sulfate, the strong absorption peak of hydrogen sulfate, the strong absorption peak of sulfate, and the weak absorption peak of sulfate, respectively. This indicates that when SO_2 is introduced into the reaction gas, sulfates and hydrogen sulfates are formed on the catalyst surface, and these substances cover the active sites on the catalyst surface, thus reducing the deNO$_x$ efficiency (Gao et al. 2013).

Conclusions

The deNO$_x$ performance of Cr-modified activated coke–supported Fe-based catalyst was investigated at 120–240 °C. With increasing Cr content, the deNO$_x$ efficiency of the 8Fe/AC catalysts is greatly increased. When the Cr addition amount reaches 6%, the catalyst has the highest SCR activity, which the NO_x conversions are more than 90% at 160–240

°C. A bigger specific surface area; higher amounts of Fe^{3+}, Cr^{3+}, and O_β; stronger reduction ability; and more acid sites are responsible for the high deNO_x activity of the 8Fe6Cr/AC catalyst. Both Brønsted acid sites and Lewis acid sites are present in the 8Fe6Cr/AC catalyst, and the L-H and E-R mechanism may contribute to the NO_x reduction for 8Fe6Cr/AC catalyst. In addition, the 8Fe6Cr/AC catalyst has high stability in the presence of 5% H_2O, but its ability of resistance to SO_2 poisoning is poor due to formed sulfates and hydrogen sulfates on the catalyst surface covering the active sites.

Funding information We greatly appreciate the financial support provided by the National Natural Science Foundation of China (Nos. 51676001 and 51376007) and the Project of Jiangsu Provincial Six Talent Peak (No. JNHB-097).

References

Amin NAS, Tan EF, Manan ZA (2003) Selective reduction of NOx with CH over Cu and Cr promoted CeO catalysts. Appl Catal B Environ 43(1):57–69

Chen Z, Yang Q, Li H (2012) Cr-MnO_X, mixed-oxide catalysts for selective catalytic reduction of NOx, with NH_3, at low temperature. J Catal 276(1):56–65

Ding K, Kong XT, Wang J (2017) Side chains of parabens modulate antiandrogenic activity: in vitro and molecular docking studies. Environ Sci Technol 51(11):6452–6460

Du XY, Li C, Zhao L (2018) Promotional removal of HCHO from simulated flue gas over Mn-Fe oxides modified activated coke. Appl Catal B Environ 232:37–48

Gao X, Liu SJ, Zhang Y (2011) Low temperature selective catalytic reduction of NO and NO_2 with NH_3 over activated carbon-supported vanadium oxide catalyst. Catal Today 175(1):164–170

Gao F, Walter ED, Karp EM (2013) Structure-activity relationships in NH_3-SCR over Cu-SSZ-13 as probed by reaction kinetics and EPR studies. J Catal 300(3):20–29

Gao F, Tang X, Yi H (2017) Promotional mechanisms of activity and SO_2, tolerance of Co- or Ni-doped MnOx-CeO_2, catalysts for SCR of NOx with NH_3, at low temperature. Chem Eng J 317:20–31

Gao L, Li C, Lu P (2018) Simultaneous removal of HgO and NO from simulated flue gas over columnar activated coke granules loaded with La_2O_3-CeO_2 at low temperature. Fuel 215:30–39

Gorji NE (2015) Degradation of ultrathin CdTe films with SWCNT or graphene back contact. Phys E 70:84–89

Huang B, Huang R, Jin D (2007) Low temperature SCR of NO with NH_3 over carbon nanotubes supported vanadium oxides. Catal Today 126(3-4):279–283

Huang Z, Hou Y, Zhu Z (2014) Study on the NO reduction by NH_3 on a SO_4^{2-}/AC catalyst at low temperature. Catal Commun 50:83–86

Kim KH, Chiu JM, Pujol J (2015) A comparative study of modified cotton biochar and activated carbon based catalysts in low temperature SCR. Fuel 156:47–53

Klukowski D, Balle P, Geiger B (2009) On the mechanism of the SCR reaction on Fe/HBEA zeolite. Appl Catal B Environ 93(1):185–193

Koehler K, Maciejewski M, Schneider H (2010) ChemInform abstract: chromia supported on titania. Part 5. preparation and characterization of supported CrO_2, CrOOH, and Cr_2O_3. J ChemInform 27(15)

Lázaro MJ, Gálvez ME, Ruiz C (2006) Vanadium loaded carbon-based catalysts for the reduction of nitric oxide. Appl Catal B Environ 68(3/4):130–138

Lin SD, Gluhoi AC, Nieuwenhuys BE (2004) Ammonia oxidation over Au/MOx/gamma-Al_2O_3- activity, selectivity and FTIR measurements. Catal Today 85(1):3–14

Lin Y, Wenju J, Liu Y (2017) Suitability of pyrolusite as additive to activated coke for low-temperature NO removal. J Chem Technol Biotechnol 93(3):690–697

Liu J, Zhao Z, Wang J (2008) The highly active catalysts of nanometric CeO_2-supported cobalt oxides for soot combustion. Appl Catal B Environ 84(1):185–195

Liu Y, Gu TT, Weng XL, Wang Y (2012) DRIFT studies on the selectivity promotion mechanism of Ca-modified Ce-Mn/TiO_2 catalysts for low-temperature NO reduction with NH_3. J Phys Chem 116: 16582–16592

Luo HC, Huang BC, Fu ML (2012) SO_2 deactivation mechanism of MnOx/MWCNTs catalyst for low-temperature selective catalytic reduction of NOx by ammonia. Acta Phys Chim Sini 28(9):2175–2182(8)

Ouzzine M, Cifredo GA, Gatica JM (2008) Original carbon based honeycomb monoliths as support of Cu or Mn catalysts for low-temperature SCR of NO: effects of preparation variables. Appl Catal A Gen 342(1-2):150–158

Pan S, Luo H, Li L (2013) H_2O and SO_2 deactivation mechanism of MnOx/MWCNTs for low-temperature SCR of NOx with NH_3. J Mol Catal A Chem 377:154–161

Phil HH, Reddy MP, Kumar PA (2008) SO_2 resistant antimony promoted V_2O_5/TiO_2 catalyst for NH_3-SCR of NOx at low temperatures. Appl Catal B Environ 78(3-4):301–308

Qiu J, Zhuang K, Lu M (2013) The selective catalytic reduction activity of Cu/MCM-41 catalysts prepared by using the Cu^{2+}-MCM-41 mesoporous materials with copper ions in the framework as precursors. Catal Commun 31:21–24

Shen B, Yao Y, Ma HQ (2011) Ceria modified MnOx/TiO_2-pillared clays catalysts for the selective catalytic reduction of NO with NH_3 at low temperature. Chin J Catal 32(11):1803–1811

Shen BX, Ma HQ, He C, Zhang XP (2014) Low temperature NH_3-SCR over Zr and Ce pillared clay based catalysts. Fuel Process Technol 119:121–129

Skarlis SA, Berthout D, Nicolle A (2014) Combined IR spectroscopy and kinetic modeling of NOx, storage and NO oxidation on Fe-BEA SCR catalysts. Appl Catal B Environ 148-149(1-2):446–465

Tang X, Hao J, Yi H (2007) Low-temperature SCR of NO with NH_3, over AC/C supported manganese-based monolithic catalysts. Catal Today 126(3):406–411

Topsoe NY (1994) Mechanism of the selective catalytic reduction of nitric oxide by ammonia elucidated by in situ on-line Fourier transform infrared spectroscopy. Science 265:1217–1219

Vishwanathan V, Jun KW, Kim JW (2004) Vapour phase dehydration of crude methanol to dimethyl ether over Na-modified H-ZSM-5 catalysts. Appl Catal A Gen 276(1-2):251–255

Wang J, Zheng Y, Liu L (2014a) Low-temperature SCR of NO with NH_3 over activated semi-coke composite-supported rare earth oxides. Appl Surf Sci 309(4):1–10

Wang JP, Yan Z, Liu LL (2014b) In situ DRIFTS investigation on the SCR of NO with NH_3 over V_2O_5 catalyst supported by activated semi-coke. Appl Surf Sci 313(13):660–669

Wang P, Sun H, Quan X (2015) Enhanced catalytic activity over MIL-100(Fe) loaded ceria catalysts for the selective catalytic reduction of NOx with NH_3 at low temperature. J Hazard Mater 301(1):512–521

Wang H, Qu Z, Dong S, Xie H (2016) Superior performance of Fe1-xWxOδ for the selective catalytic reduction of NOx with NH_3: interaction between Fe and W. Environ Sci Technol 50(24):13511–13519

Wang A, Guo Y, Gao F (2017a) Ambient-temperature NO oxidation over amorphous CrOx-ZrO_2, mixed oxide catalysts: significant promoting effect of ZrO_2. Appl Catal B Environ 202:706–714

Wang L, Wang Z, Cheng X (2017b) In situ DRIFTS study of the NO+CO reaction on Fe-Co binary metal oxides over activated semi-coke supports. RSC Adv 7(13):7695–7710

Wu Z, Sheng Z, Liu Y (2011) Deactivation mechanism of PtOx/TiO(2) photocatalyst towards the oxidation of NO in gas phase. J Hazard Mater 185(2-3):1053–1058

Xing Y, Li LL, Lu P (2017) Simultaneous purifying of HgO, SO_2, and NOx from flue gas by Fe^{3+}/H_2O_2: the performance and purifying mechanism. Environ Sci Pollut Res Int 25(7):6456–6465

Yang S, Guo Y, Yan N (2011) Nanosized cation-eeficient Fe-Ti spinel: a novel magnetic sorbent for elemental mercury capture from flue gas. ACS Appl Mater Interfaces 3(2):209–217

Yang S, Liu C, Chang H (2013) Improvement of the activity of γ-Fe_2O_3 for the selective catalytic reduction of NO with NH_3 at high temperatures: NO reduction versus NH_3 oxidization. Ind End Chem Res 52(16):5601–5610

Yang R, Huang H, Chen Y (2015) Performance of Cr-doped vanadia/titania catalysts for low-temperature selective catalytic reduction of NOx with NH_3. Chin J Catal 36(8):1256–1262

Yang NZ, Guo RT, Pan WG (2016a) The deactivation mechanism of Cl on Ce/TiO_2 catalyst for selective catalytic reduction of NO with NH_3. Appl Surf Sci 378:513–518

Yang S, Qi F, Xiong S (2016b) MnOx, supported on Fe-Ti spinel: a novel Mn based low temperature SCR catalyst with a high N_2, selectivity. Appl Catal B Environ 181:570–580

Zhang X, Cui H, Chen D (2018) Electronic structure and H_2S adsorption property of Pt_3, cluster decorated (8,0) SWCNT. Appl Surf Sci 428:82–88

Zhu L, Zhang L, Qu HX, Zhong QA (2015) Study on chemisorbed oxygen and reaction process of Fe-CuOx/ZSM-5 via ultrasonic impregnation method for low-temperature NH_3-SCR. J Mol Catal A Chem 409:207–215

Zhu B, Yin S, Sun Y (2017) Natural manganese ore catalyst for low-temperature selective catalytic reduction of NO with NH_3 in coke-oven flue gas. Environ Sci Pollut Res 24(31):24584–24592